FLOW AND HEAT TRANSFER PREDICTIONS FOR FILM-COOLING FLOWS USING LARGE EDDY SIMULATIONS

MAYANK TYAGI, SUMANTA ACHARYA
Mechanical Engineering Department
Louisiana State University, Baton Rouge, LA

Abstract

Large eddy simulations are performed to study the flow physics and heat transfer for the film-cooling of gas turbine blade surface. The coolant jet issues out from a cylindrical delivery tube into the mainflow at an inclination angle of 35°. The Reynolds number based on the jet velocity and the diameter of the delivery tube is approximately 11100. The jet to mainflow velocity ratio is 0.5. Heat transfer calculations are also performed simultaneously to study the mixing of the passive scalar with the mainflow, evaluate film-cooling effectiveness and heat transfer predictions on the blade surface. The parameters in the simulation correspond to the experiments performed at UTRC (Lavrich and Chiappetta, 1990)

1. Introduction

Advanced gas turbines are designed to operate at high turbine inlet temperatures. Increased temperatures improve the second law efficiency as well as the specific thrust obtained by the turbines. This poses a challenge to design better and efficient cooling methodology for gas turbine blades in the stages after the combustor. Film-cooling is used to maintain the turbine blade temperature below their melting point for the increased blade life. In film-cooling, coolant jets are injected at an angle into the hot mainflow that deflects these coolant jets over the blade surface to provide a coolant film coverage. However, the increased amount of coolant injection can deteriorate the aerodynamic performance and the gas path temperature drastically. Therefore, the amount of coolant should be optimal.

There is enormous amount of literature on the numerical studies done for a jet-in-crossflow configuration (Acharya et al, 2001). Most of the studies employed two-equation turbulence models with varied degree of success in predicting the flow field and heat transfer. Earlier LES studies of jet-in-crossflow flow situations (Jones and Wille, 1996, Yuan et al., 1999, Tyagi and Acharya, 1999) were performed for normal injections and high blowing ratios. In this study, a computational domain was chosen that represented the experiments conducted at UTRC. In general, the RANS calculations under-predict the lateral spread and mixing of the jet while they over-predict the vertical penetration of the coolant jet. In figure 1, predictions of the transverse shear stress component $u'w'$ that is responsible for the lateral spread are shown for Reynolds Averaged Navier Stokes (RANS) calculations using two-equation turbulence model, second moment closure model and previous LES studies for a square jet injected normally into the crossflow (Walters and Leylek, 1997, Tyagi and Acharya,

1999). Clearly, RANS modeling either at two-equation level or at the second moment level is inaccurate for this stress component while LES can capture the flow physics well.

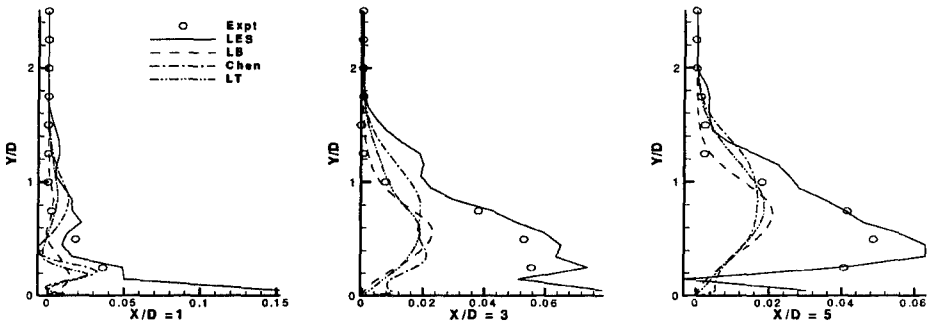

Figure 1 Transverse shear stress ($u'w'$) along Z/D = -0.5. RANS vs LES predictions. The experimental data is from Ajersch et al (1995).

2. Governing Equations and Computational Method

The non-dimensional governing equations for conservation of mass, momentum and energy for an incompressible Newtonian fluid in LES methodology are as follows

$$\frac{\partial U_j}{\partial x_j} = 0$$

$$\frac{\partial U_i}{\partial t} + \frac{\partial U_i U_j}{\partial x_j} = -\frac{\partial p}{\partial x_i} + \frac{1}{\mathrm{Re}} \frac{\partial^2 U_i}{\partial x_j^2} + \frac{\partial \tau_{ij}}{\partial x_j} + f_i$$

$$\frac{\partial \Theta}{\partial t} = [1-\Phi]\left(-U_j \frac{\partial \Theta}{\partial x_j} + \frac{1}{\mathrm{Re}\cdot \mathrm{Pr}} \frac{\partial^2 \Theta}{\partial x_j^2} + \frac{\partial q_j}{\partial x_j} \right) + \Phi \frac{\Lambda}{\mathrm{Re}\cdot \mathrm{Pr}} \frac{\partial^2 \Theta}{\partial x_j^2}$$

where U_i is the filtered velocity field, f_i is the body force terms arising due to immersed solid surfaces, $\Theta = \dfrac{T - T_\infty}{T_j - T_\infty}$ where T_j is the coolant jet temperature and T_∞ is the mainflow temperature, Λ is the ratio of thermal diffusivity of the immersed solid to thermal diffusivity of the fluid and Φ is the indicator function for solving the solving the unsteady diffusion problem in the immersed solid. The indicator function is 1 inside the solid and zero everywhere else. The SubGrid Scale (SGS) stress tensor and SGS scalar flux vector are given by τ_{ij} and q_j respectively. In this study, Dynamic Mixed Model (DMM) is used to model these SGS stress tensor and scalar flux vector (Moin et al., 1991, Vreman et al., 1994). The box filters are used in the Germano identity for the calculation of

dynamic coefficient and for the calculation of Leonard stresses. The dynamic coefficient is test filtered to avoid numerical instabilities.

The momentum equations are solved using projection method. The temporal scheme is explicit second order accurate Adams-Bashforth scheme. The spatial descretization is done using fourth order central finite-difference schemes for all the terms except the convective term $\left(\frac{\partial U_\alpha U_\alpha}{\partial x_\alpha}\right)$ that is upwind-differenced with a third accurate scheme. The pressure-Poisson equation is solved using a direct solver based on matrix diagonalization. The Laplacian operator is approximated using 4-2 formaulation i.e. the gradient operator is fourth order central difference operator and the divergence operator is second order accurate central difference operator. All the terms in energy equation are fourth order centrally differenced.

3. Problem Description

A uniform grid of 172×102×42 is used to model the computational domain of size 17D×5D×4D, where D is the diameter of the coolant jet delivery tube. The film-cooled surface is placed at 1.5D from the bottom of the computational domain. The center of the jet injection hole at the film-cooled surface is 5D downstream from the inlet plane. The jet delivery tube is simulated as a cylindrical surface inclined at 35° in the streamwise direction (X) using Immersed Boundary Method. A crossflow-stagnation type plenum is simulated in this study for the coolant supply. The top wall for the plenum is placed at 0.5D from the bottom of the computational domain. The bottom plane of the computational domain is treated using symmetry boundary conditions. Top boundary of the computational domain is treated as freestream boundary. At the inlet, fully developed turbulent profile is specified. At the outflow, a convective boundary condition is used where the convection speed is obtained from the mass flux balance. The spanwise direction (Z) is assumed to be periodic.

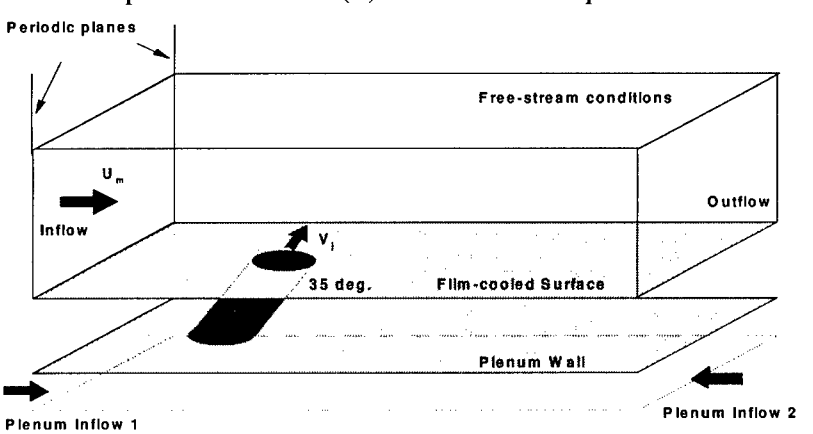

Figure 2 Schematic of the computational domain

4. Results and Discussion

The experiments were conducted with a large tube-length (approx. 5.5D) and a can-type plenum. However, in this study, the plenum is simulated as a stagnation flow field below the jet-delivery tube. The mass flow rate into the plenum is such that the velocity ratio of 0.5 is achieved at the coolant hole exit. The jet-delivery tube is short (approx. 1.74D). These changes are made to simulate a reasonable computational domain that retains all the essential physics. Such discrepancies are not expected to change the flow field dynamics and heat transfer in this flow situation drastically.

FLOW FIELD DESCRIPTION

There is a recirculation region inside the tube at the leeward surface (Figure 3a). This effect has been reported in earlier RANS studied (Walters and Leylek, 1997). The stagnation flow field below the jet delivery tube as well as the recirculation regions in the tube are observed in figure 3b. The development of the vorticity field inside the delivery tube leads to complex internal structure to the counter-rotating vortex pair (CVP) or the kidney vortex in this flow situation (Fric and Roshko, 1994, Andreopoulos and Rodi, 1984). The recirculation region behind the jet on the wall is also noted.

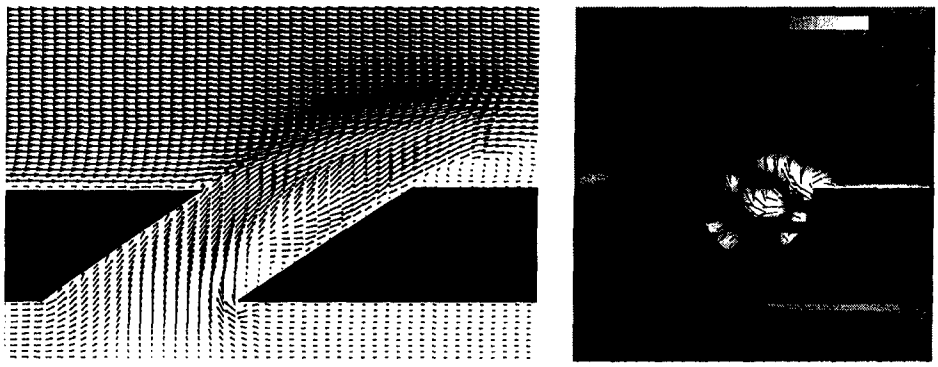

Figure 3 Details of the velocity field inside the coolant jet delivery tube

In figure 4a-c, the instantaneous vorticity field components are presented on the jet-centerplane (Z/D = 0.0). The streamwise component of vorticity, ω_x indicates the location of the lobes of CVP and the intertwining of this vorticity component is an indicator of crossplane mixing. The contours of ω_y correspond to the upright wake vortices that are shed into the wake of the deflected jet. The contours of ω_z show the vorticity generated inside the tube around the recirculation region near the plenum, is shed along with the vorticity generated at the leeward edge of the coolant jet. The interaction of the vorticity generated at windward edge of the coolant jet inside the delivery tube and the oncoming boundary layer vorticity is also observed. The delivery tube vorticity dynamics gives rise to complex and unsteady CVP.

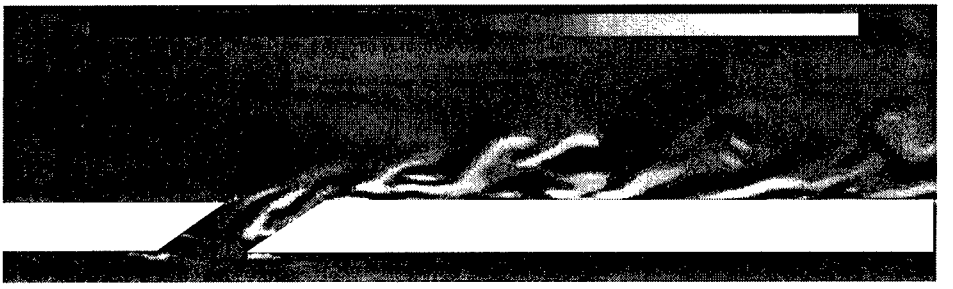

a) ω_x

b) ω_y

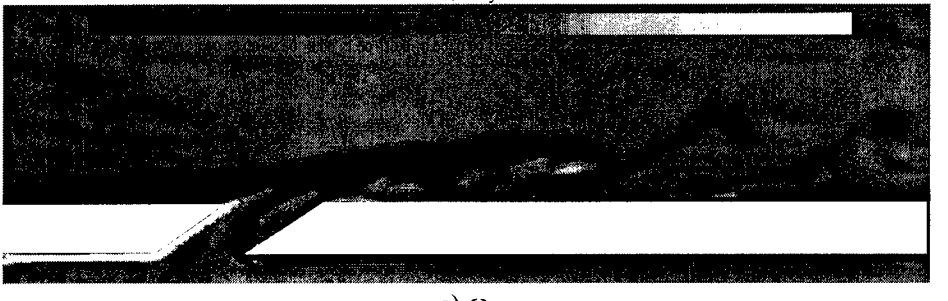

c) ω_z

Figure 4 Instantaneous vorticity field components (a-c) on the jet-centerplane.

In figure 5a-c, the instantaneous vorticity field components are presented over the film-cooled surface (Y/D = 1.5). The streamwise component of vorticity, ω_x around the periphery of the injection-hole shows the origin of the CVP. The contours of ω_x are aligned with the streaks formed due to the entrainment of the crossflow into the wake region. The contours of ω_y show a complicated structure of the coolant jet inside the injection hole. The upright wake vortices are shed from the edges of the coolant jet due to the interaction with the crossflow, entrained into the wake region and convected downstream. The contours of spanwise vorticity component, ω_z show the vorticity generated along the delivery tube walls. This component plays an important role in changing the structure of CVP in the near field of the jet.

a) ω_x

b) ω_y

c) ω_z

Figure 4 Instantaneous vorticity field components (a-c) on the film-cooled wall surface.

PASSIVE SCALAR (TEMPERATURE) FIELD DESCRIPTION

The details of instantaneous temperature field are given at several section of the computational domain (figure 6). The centerplane corresponds to Z/D = 0.0 and shows the mixing of the mainflow and the coolant jet. The coolant jet temperature drops in the downstream direction, however the coherent structures in the wake region retain their scalar value further (Fig. 6a). The temperature distribution corresponding to adiabatic wall boundary conditions corresponds to film-cooling effectiveness too (fig. 6b). The coolant jet provides good coverage immediately downstream of the injection hole, however the film-cooling effectiveness decreases monotonically in the wake region along the centerplane. The development of the coolant jet along the streamwise direction is shown at three different X/D locations (fig 6c-e). The coolant jet is observed to have a well defined kidney shaped structure (Andreopoulos and Rodi, 1984, Fric and Roshko, 1994). The crossplane mixing of scalar leads to the decrease in scalar value in the core of coolant jet at downstream stations. Moreover, the jet is attached to the surface near the centerplane but is lifted off below the lobes of the kidney vortex.

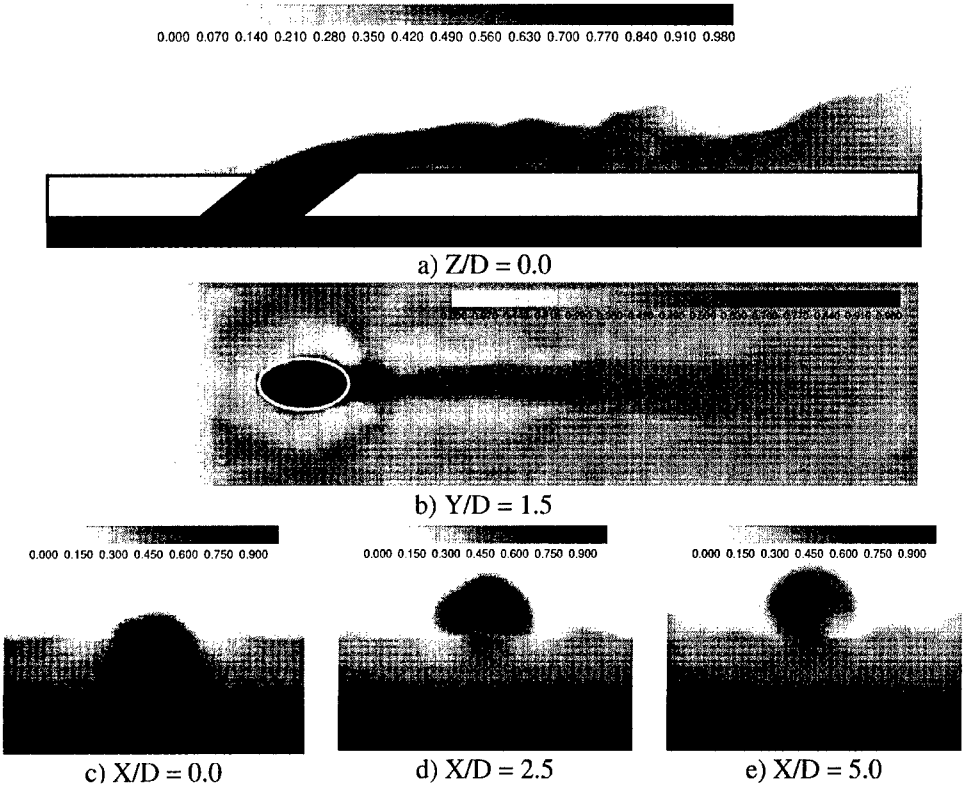

Figure 6 Instantaneous temperature field at different computational domain sections.

5. Conclusion

Large eddy simulations were performed for a simplified geometry representing film-cooling of a gas turbine blade surface. The heat transfer calculations were performed in a conjugate heat transfer mode to study the heat transfer on the film-cooled wall. The plenum was simulated by a stagnation flow field. The unsteady dynamics inside the coolant jet delivery tube showed complex internal structure of the CVP. The coherent vortices observed were in agreement with the experiments conducted by various researchers (Kelso et al., 1996, Haven and Kurosaka, 1997, Fric and Roshko, 1994). The heat transfer results showed the unsteady mixing of the coolant with crossflow and the instantaneous film-cooling effectiveness. The detailed comparison of film-cooling effectiveness, mean flow field and the turbulence statistics will be presented in the future.

References

Acharya, S., Tyagi, M., and Hoda, A. (2001) Flow and heat transfer predictions for film cooling, *Heat transfer in gas turbine systems*, Annals of the New York Academy of Sciences, Vol. 934, pp. 110-125.

Ajersch, P., Zhou, J.M., Ketler, S., Salcudean, M. and Gartshore, I. (1995), Multiple jets in a crossflow: detailed measurements and numerical simulations, *ASME-95-GT-9.*

Andreopoulos, J. and Rodi, W. (1984), Experimental investigation of jets in a crossflow, *J. Fluid Mech.*, Vol. 138, pp.93-127.

Fric, T.F. and Roshko, A. (1994), Vortical structure in the wake of a transverse jet, *J. Fluid Mech.*, Vol. 279, pp. 1-47.

Haven, B.A. and Kurosaka, M. (1997), Kidney and anti-kidney vortices in crossflow jets, *J. Fluid Mech.*, Vol. 352, pp. 27-64.

Jones, W.P. and Wille, M. (1996), Large eddy simulations of a round jet in crossflow, *Engineering turbulence modeling and experiments* 3, pp. 199-209.

Kelso, R.M., Lim, T.T. and Perry, A.E. (1996), An experimental study of round jets in crossflow, *J. Fluid Mech.*, Vol. 306, pp. 111-144.

Lavrich, P.L., and Chiappetta, L.M. (1990) An investigation of jet in a cross flow for turbine film cooling applications, *UTRC Report* No. 90-04.

Moin, P., Squires, K., Cabot, W. and Lee, S. (1991), A dynamic subgrid-scale model for compressible turbulence and scalar transport, *Phys. Fluids* A 3, Vol. 11, pp. 2746-2757.

Tyagi, M. and Acharya, S. (1999), Large eddy simulations of rectangular jets in crossflow: Effect of hole aspect ratio, *Recent advances in DNS and LES*, Ed. Knight and Sakell, pp. 431-442.

Vreman, B., Guerts, B. and Kuerten, H. (1994), On the formulation of the dynamic mixed subgrid scale model, *Phys. Fluids*, Vol. 6, pp. 4057-4059.

Walters, D.K. and Leylek, J.H. (1997), A detailed analysis of film-cooling physics part 1: streamwise injection with cylindrical holes, *97-GT-269.*

Yuan, L.L., Street, R.L. and Ferziger, J.H. (1999), Large eddy simulations of a round jet in crossflow, *J. Fluid Mech.*, Vol. 379, pp. 71-104.